

Simulation of the vibration generated by entry and exit to/from a spall in a rolling element bearing

Nader Sawalhi and Robert B Randall

School of Mechanical and Manufacturing Engineering

The University of New South Wales, Sydney 2052, Australia

Telephone +61 2 9385 5564

n.sawalhi@unsw.edu.au

PACS: 43.40.At

ABSTRACT

In bearing prognostics it is important to be able to feed back information on the current size of a spall, in order to determine the rate of progress of the fault, and make better estimates of remaining useful life (RUL). A method has recently been developed to measure the time delay between the entry and exit events so as to be able to estimate the fault size. It was found that the two events are quite different, the entry being a step response and the exit an impulse response, with very different strength and frequency content. A range of signal processing techniques were developed to enhance the two signatures so as to better measure the time delay between them, but the estimates were affected to some extent by the processing parameters. In the current paper, the entry and exit events are simulated as modified step and impulse responses with precisely known starting times, so as to be able to determine the effects of various simulation and signal processing parameters on the estimated delay times. One of the ways of determining the delay time is by using the cepstrum to measure the "echo delay time", and already the simulation has been found useful in pointing to artefacts associated with the cepstrum calculation which affect even the simulated signals and have thus prompted modifications of the processing of real signals. The paper presents the results of the study into the effects of simulation parameters such as dominant frequency content, and processing techniques such as optimum choice of wavelets used to choose a frequency band to balance the entry/exit events.

INTRODUCTION

A number of authors [1-6] have contributed to the modelling of bearing fault signals. Nevertheless, most of these models were directly affected by the way in which the bearing fault manifests itself in the high frequency region and how it appears in the envelope spectrum. Little attention has been given to the observation of Epps & McCallion [7], who found that for an outer race notch fault there is a negative ramp in the acceleration signal (step response) which represents the entry of the rolling elements into the fault followed by the response of the bearing system (impulse response) when the rolling element strikes the other edge of the fault. These two events can be seen clearly in figure 1.

Epps & McCallion also found the separation between the Point of Entry and the Point of Impact to be in proportion to the size of the fault; which has also been observed from the results of the seeded faults measured on the UNSW fan test rig [8], so this could be a very useful trending parameter. Although the step response (seen to excite low frequencies) is usually undetected in the signal (possibly because of the presence of background noise and gear vibration, and the use of the high resonance frequency technique, which suppresses the low frequency components) it is important to include it in a simulation model.

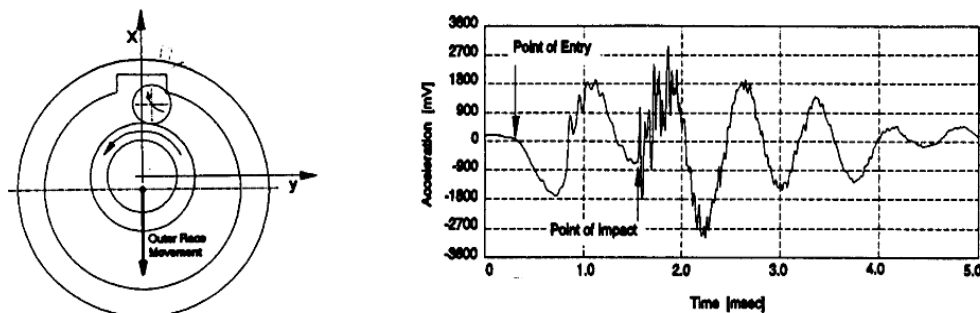


Figure 1 Left: Model of rolling element travelling into a fault. Right: A typical measured response [7]

A typical result for an outer race fault [8] is shown in figure 2, which shows the entry as a step function, while that at the exit as an impulse. This has also been found to be in good correspondence with the observations of reference [7].

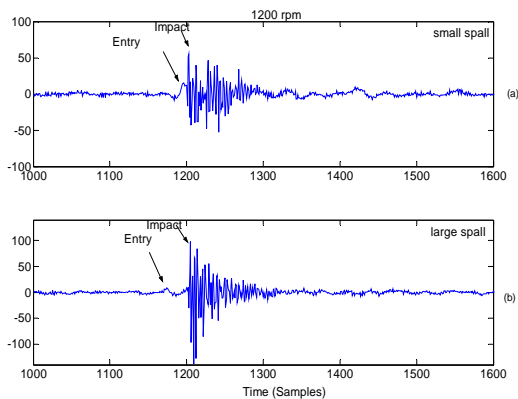


Figure 2 Comparison of the raw accelerometer signals for the small (0.6 mm) and large (1.2 mm) outer race faults [8].

On entry, the rolling element would roll over the edge with a fixed radius of curvature (equal to that of the rolling element), but this sudden change in curvature would represent a step in acceleration. On exiting the spall, the centre of the rolling element would have to change direction suddenly, this representing a step in velocity or an impulse in acceleration.

This paper presents an analytical model for an outer race rolling element bearing fault, which comprises both the step and impulse responses. The measured and simulated results are compared and subjected to the same processing techniques. Results show the success of the simulation model and its ability to match the measured results. This is a major contribution to the field of rolling element bearing simulation.

ANALYTICAL SIMULATION MODEL

An outer race fault is generally initiated in the region of the load zone and the defect resembles a depression in the raceway. As a rolling element rolls in and out of the fault, it will de-stress and re-stress respectively. The rolling element drops into the depression and most of the load will be transferred to the adjacent rollers or balls.

Based on the observations from [7,8], the entry into the fault appears like a step response, with mainly low frequency content, while the impact on exit excites a much broader band impulse response as explained in the Introduction.

A single degree of freedom (SDOF) impulse response (in the form of a decaying sinewave) can be generated analytically using equation (1).

$$y_1 = e^{(-t/\tau)} \times \sin(2 \times \pi \times f \times t) \quad (1)$$

where f is the natural frequency (Hz) and τ is the damping time constant (s).

To avoid aliasing, it is advantageous to generate the signal (time vector [t]) using a very high sampling frequency and then resample it at a lower rate (using the Decimate function in Matlab® for instance). In order to generate an impulse representative of that obtained from the impact of the rolling element with the trailing edge, the resonant frequency (f) was set to 6500 Hz, while the time constant (τ) was set to

0.001s. The signal was generated at a sampling frequency of 250 kHz, which was then decimated by 10, i.e. the final sampling frequency of the signal (f_s) is 25 kHz. The impulse generated using equation (1) with the above stated setup is shown in figure 3.

Meanwhile, a step response was generated analytically using equation (2) as follows:

$$y_2 = \underbrace{e^{(-t/(3 \times \tau))} \times -\cos(2 \times \pi \times (f/6) \times t)}_1 + \underbrace{e^{(-t/(5 \times \tau))}}_2 \quad (2)$$

Note the step response (y_2) is made up of two main parts. The first represents a decaying negative cosine, while the second is an exponential function to firstly introduce a DC shift of the first part (thus creating the step response) and to secondly cause a decay of the step response. In actual measured signals, the step response decays because of the AC coupling of the accelerometer. The resonant frequency for the step response has been selected as 1083.8 Hz, i.e. one sixth of the resonant frequency of the impulse response. The damping time constants have been selected to give a reasonable damping in the response (guided by some of the measurements). The step response is plotted in figure 4.

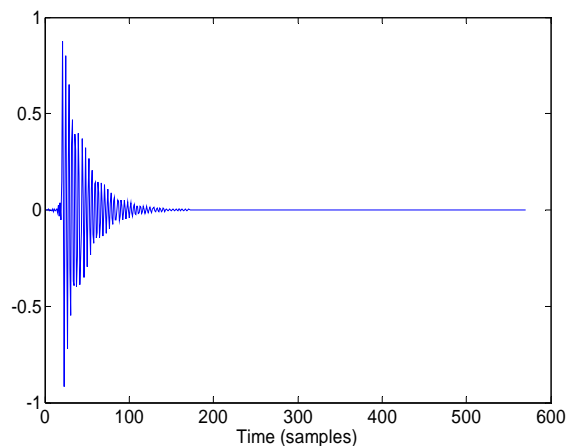


Figure 3 Impulse response generated using equation (1), with a delay at the beginning.

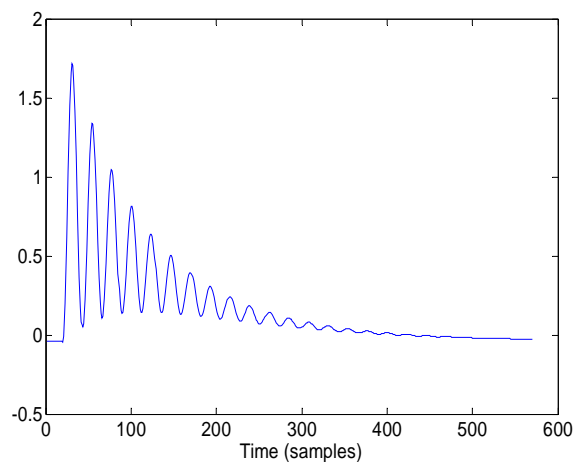


Figure 4 Step response generated using equation (2), with a delay at the beginning. $f_s = 25$ kHz, resonant frequency = 1083.3 Hz,

A step train and an impulse train were created with 2% spacing variation as shown in figure 5.a and 5.b respectively. The step function (5.a) is a scaled version of the one shown in figure 4 (divided by 20) and has a shift of 30 samples (fault width). This was then added to the impulse function (5.b) to represent the faulty signal of a bearing with an outer race spall as illustrated in figure 5.c. The effect of adding some noise to the signal (signal to noise ratio (SNR) of 20 dB) is illustrated in figure 5.d. Note that the signal presented in figure 5.b (impulse response) is the one generally shown when discussing the vibration response of spalled rolling element bearings (e.g. references 1,2,5 and 6).

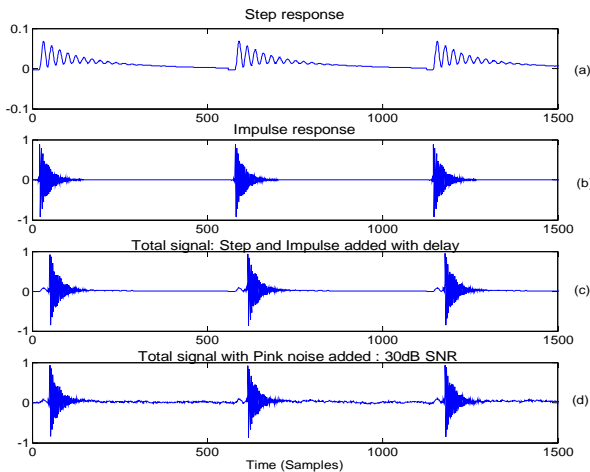


Figure 5 a) Step response (b) Impulse response (c) step response scaled and added to the impulse with a delay of 30 samples (d) signal (c) with a SNR of 30 dB

SIMULATED AND EXPERIMENTAL RESULTS

THE UNSW BLADED TEST RIG

A set of measurements was carried out on a bladed disk test rig at the Vibration and Acoustics Lab at UNSW. The test rig has 19 flat blades attached to a disk, which is mounted on a shaft. The shaft is supported by two self-aligning, double row ball bearings (NACHI 2206 GK), which are mounted on sleeves and are contained within Plummer blocks. The test rig is driven by a variable speed motor, coupled to the test rig via a multi-rib V belt of ratio 1:1.

Notch faults were introduced into the outer and inner race of the double-row ball bearing (Fig. 6). This was performed using electric spark erosion to generate a gap in the race to resemble a spall. The acceleration response from the test rig containing a seeded notch fault in the inner race (width 1.1 mm i.e. 31 samples) was compared to that of the simulation model. Vibration signals were collected using an accelerometer positioned on the top of the free end Plummer block above the defective bearing. The 10s (655360 sample) signals were sampled at 65.536 kHz. A once-per-rev tachometer is placed next to the coupling.

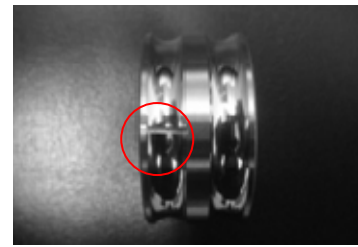


Figure 6 Notch fault introduced to the inner race

SIGNAL PROCESSING APPROACHES

Figure 7 illustrates the steps included in processing the signal to enhance the step and impulse responses resulting from the entry and exit of the spall [8].

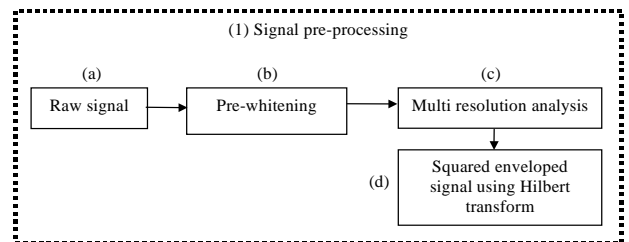


Figure 7 signal processing algorithm to enhance both the step and impulse responses (joint treatment) [8]

As evident from figures 1 and 2, and the simulation model of figure 5.d, the impact event is more energetic than the entry event, and comprises a wider frequency range, so the first step in processing the signals is to pre-whiten it using AR methods (step b) [9] The pre-whitened signal was then filtered using a filter bank based on complex Morlet wavelets [10], (a coarse filter bank with one filter/octave was selected). The filtered signal that best enhances the two events is selected and its squared envelope signal is calculated using the Hilbert transform [5]. Note that an alternative approach to isolate the two events (Separate treatment) has been proposed earlier with good results [11]. A summary of this processing is shown in figure 8.

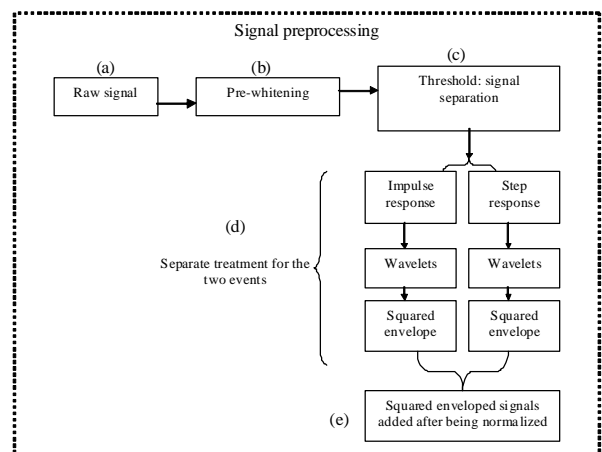


Figure 8 Signal pre-processing to separately enhance the step and impulse responses

For quantifying the fault (fault size extraction), use was made of the properties of the cepstrum to determine the delay between two similar events (i.e. an echo). The real cepstrum was used because it is not sensitive to whether the “echo” is stronger or weaker than the original. It is defined as the inverse Fourier transform of the logarithm of the magnitude of

an autospectrum [12] Averaging could be done over individual cepstra, or by forming an averaged autospectrum and calculating the cepstrum only once.

The results from joint and separate treatment are shown next for the simulated and measured results. Results are shown for inner race faults, in sections where the fault is in the load zone, but similar results were obtained for outer race faults.

RAW SIGNAL COMPARISON

The simulated result of figure 5.d can be compared to an actual measured signal from the test rig as seen in figure 9. The similarities are quite noticeable. Both signals are dominated by the impulse response. The presence of the step response is almost buried in the noise and barely noticeable.

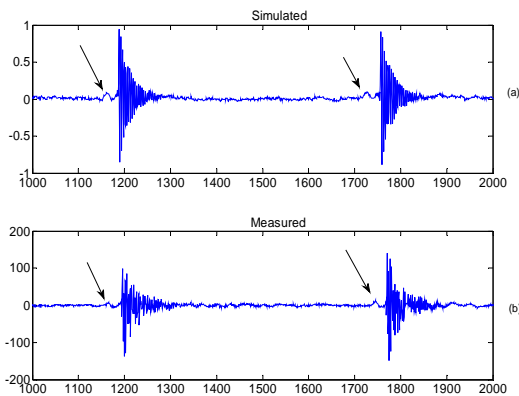


Figure 9 (a) Simulated signal (delay = 30 (fault size), SNR =15) (b) Measured signal

PROCESSED SIGNALS

Joint treatment

Figure 10 shows a zoomed presentation of three simulated entry-exit events during the different stages of processing. This is further illustrated and compared to the processing of one measured entry-exit event in figure 11. In 10.b, the signal is first pre-whitened. This signal is then processed using complex Morlet wavelets where a scale is selected to filter the signal so as to give balanced presentation of the step and impulse responses. The result is shown in figure 10.c and 11.c

The signals in 10.c and 11.c were then enveloped using a Hilbert transform process. The similarity to the measured signal is again noticeable. However, pre-whitening in the measured signals seems to give a better improvement compared to that in the simulated signals. This is because the actual signal has a number of resonances while single representative ones were selected for the simulations. Another important observation here is the presence of a ‘double impulse’ in the measured signal. This is thought to be the result of a beat in the signal due to nonlinearity in the stiffness. In the simulated model this is not clearly observable because the model only has a single constant stiffness representing a typical excited high resonance frequency.

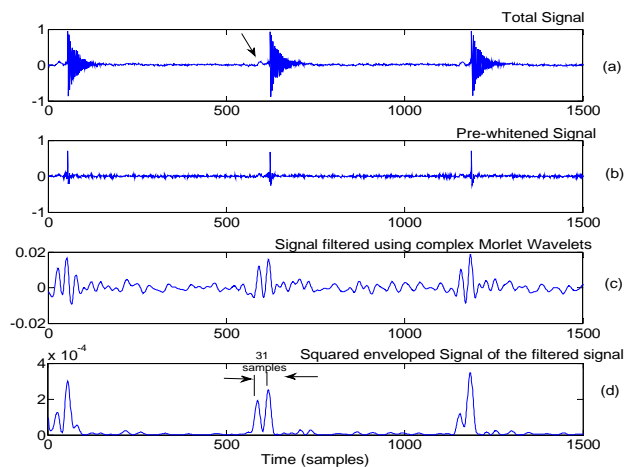


Figure 10 Joint treatment processing for simulated signals (a) Total signal (b) Prewhitened (c) Filtered using Complex Morlet wavelet (d) Squared enveloped signal using Hilbert transform

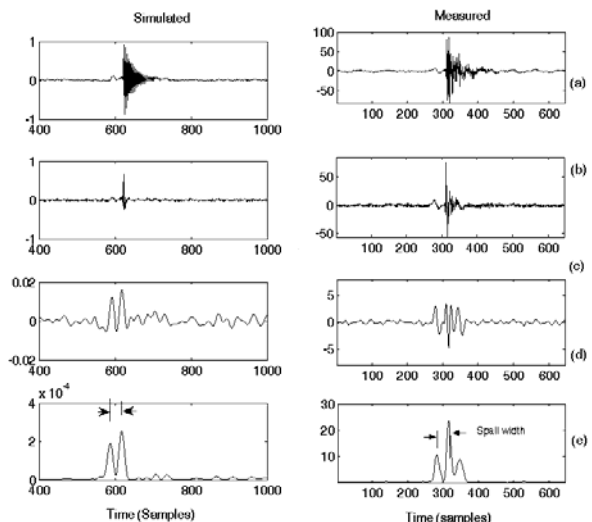


Figure 11 Simulated and measured signal comparisons under the same processing techniques (a) Total signal (b) Prewhitened (c) Filtered using Complex Morlet wavelet (d) Squared enveloped signal using Hilbert transform

During the processing of the simulated signals, it was noticed that because the bandwidth of the Morlet wavelets is a whole octave, the selection of the centre frequency of the filter plays an important role in enhancing the step response and equalizing the strength of both for further processing. This can be seen by comparing the filtered signals in figure 12, which shows the filtering results using slightly different filters. The 1st column, with the highest centre frequency of 4464.29 Hz, provides a much better enhancement of the step response compared to the processing using the second set of filters (2nd column with the highest filter centre frequency of 6250). This can be seen clearly on the enveloped signals using the different scales as presented in figure 13. When using a filter with a centre frequency of 279.02, the spacing between the step and impulse responses is much clearer compared to using a filter with a centre frequency of 390.63 Hz.

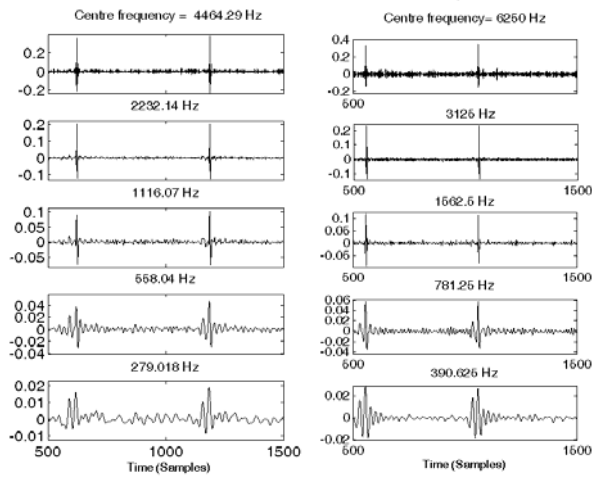


Figure 12 processing the simulated signal using Wavelets with different scales and centre frequencies.

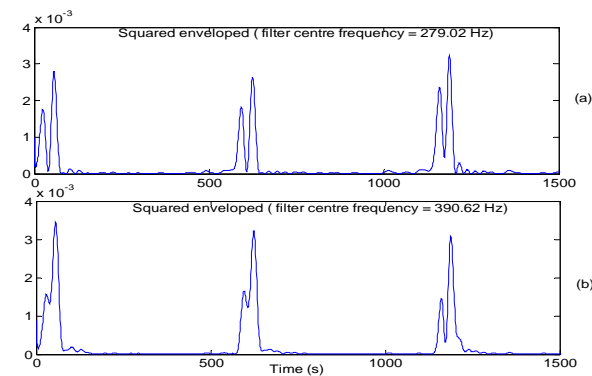


Figure 13 Squared enveloped signals for filtered signals using slightly different centre frequencies (a) Centre frequency of 279.02 Hz (b) Centre frequency of 390.52 Hz

The estimation of the size of the fault has been carried out using the cepstrum. Each event (entry/exit) is windowed and is then filtered using MED (stands for Minimum Entropy Deconvolution [13]) to sharpen the step and impulse responses. The fault size (30 samples) estimation (figure 14.a) for the simulated data has good agreement and consistency with the reported observations from the measured signals as can be seen in figure 14.b (31 samples).

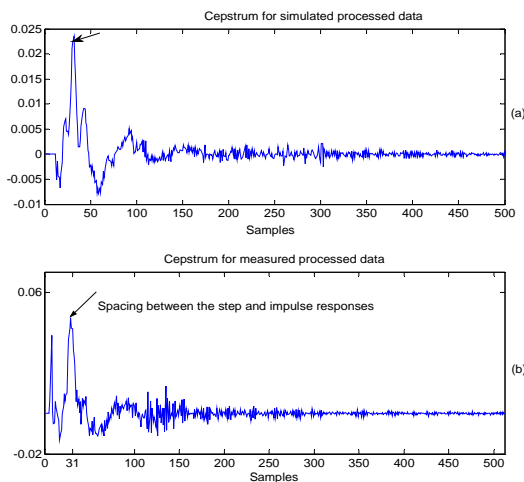


Figure 14 Cepstra comparison for the processed signal (a) simulated (b) measured

The inspection of the logarithmic spectrum (used to generate the cepstrum) as shown in figure 15, highlighted a limitation associated with processing the two different events simultaneously (step/impulse responses which have different base widths). The first noticeable effect is the limitation of the useful frequency range of the spectrum, while the second relates to limiting the dynamic range as shown by the dotted red line of figure 15. Note that large negative spikes in the log spectrum have a large effect on the cepstrum but are physically meaningless.

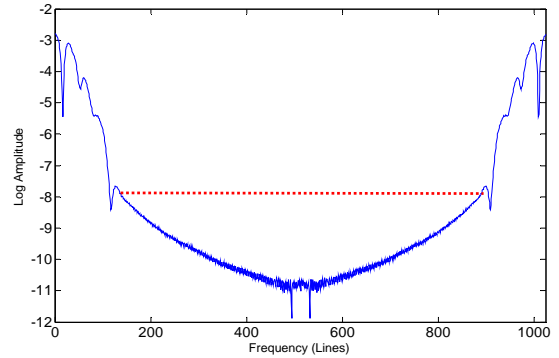


Figure 15 Log Spectrum of one step-impulse event. Red dotted line suggest a possible limit for the dynamic range

When the dynamic range of the log spectrum was limited to that shown by the red dotted line, the cepstrum estimate was shown to improve in terms of providing a much smoother estimate on the whole range and a slight improvement around the peak of interest (around the size of the fault). These effects can be seen by inspecting figure 16. The effects on the measured data are expected to be much more prominent

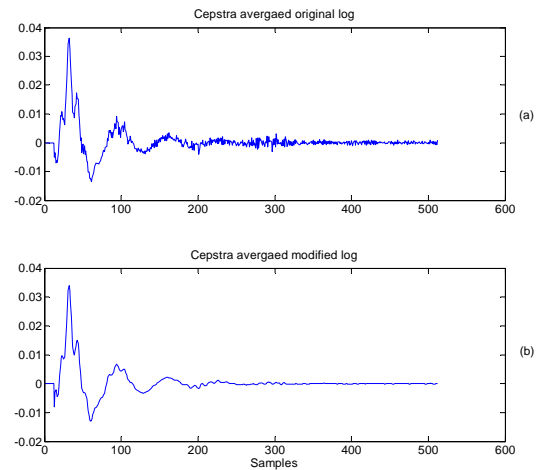


Figure 16 (a) Cepstrum averaged estimate on the original log spectrum (b) Cepstrum averaged estimate on the modified (dynamic range limited) log spectrum

Separate treatment

Figure 17 shows the separation of the step and impulse response for the pre-whitened simulated signals. The measured corresponding figure is shown in figure 18.

Figures 19 and 20 shows the separate treatment of each response, using wavelets and then Hilbert transform. The enhancement is clear and the result of normalizing each enhanced response and putting the two back in one signal is shown in figure 21

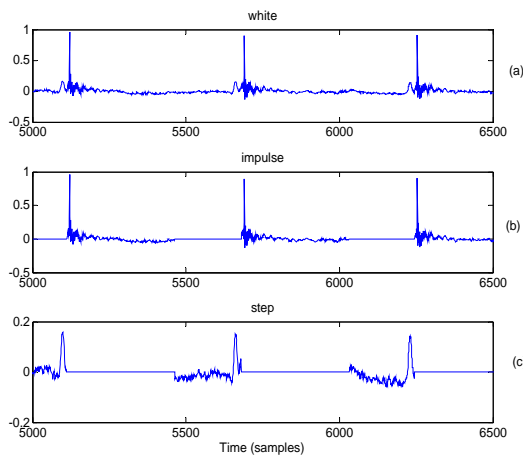


Figure 17 separating the total simulated response into step and impulse responses (a) Pre-whitened signal (b) Impulse response (c) Step response

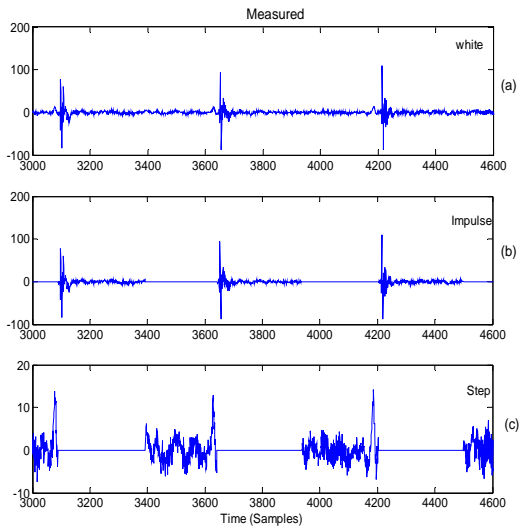


Figure 18 separating the total measured response into step and impulse (a) Pre-whitened signal (b) Impulse response (c) Step response

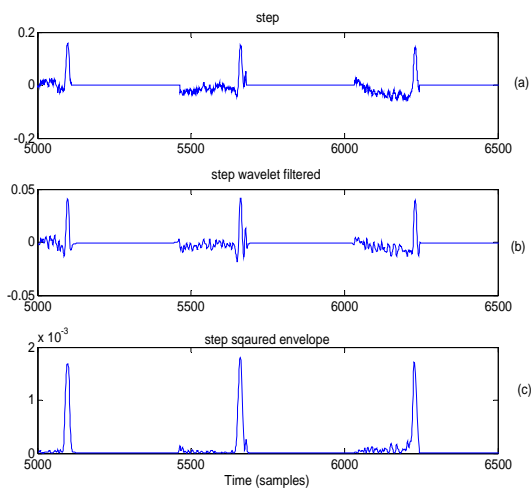


Figure 19 (a) step response (b) step response filtered using wavelets (c) signal b squared enveloped

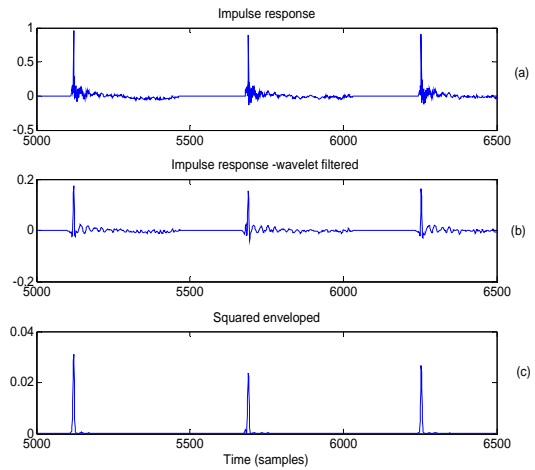


Figure 20 (a) Impulse response (b) Impulse response filtered using wavelets (c) signal b squared enveloped

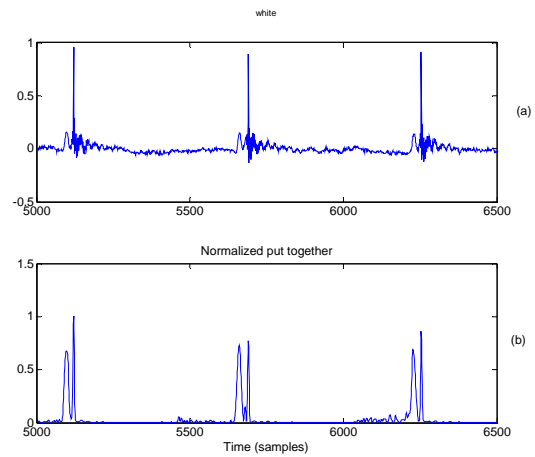


Figure 21 (a) pre-whitened simulated signal (b) enhanced and normalized step and impulse responses

Note that the assembled two events are now very clear and arithmetic calculations can be used to estimate the size of the spall. If the Cepstrum were used to estimate the size, the artefacts pointed out earlier are expected to be more evident due to the fact that the impulse now almost resembles a delta function while the step has a wider base. The log spectrum of one step-impulse response of figure 21.b is shown in figure 22.

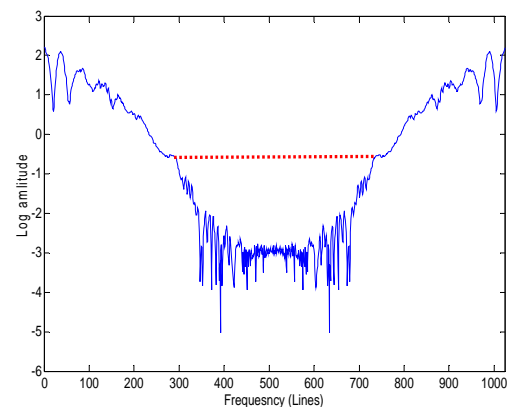


Figure 22 Log Spectrum of one step-impulse event. Red dotted line suggest a possible limit for the dynamic range

The cepstrum estimates associated with the actual spectrum and the modified one are shown in figure 23. The limitation of the dynamic range has now a clearer effect in enhancing the use of the cepstrum to estimate the size. The estimate (27 samples) is less accurate than the one obtained from the joint treatment (32 samples)

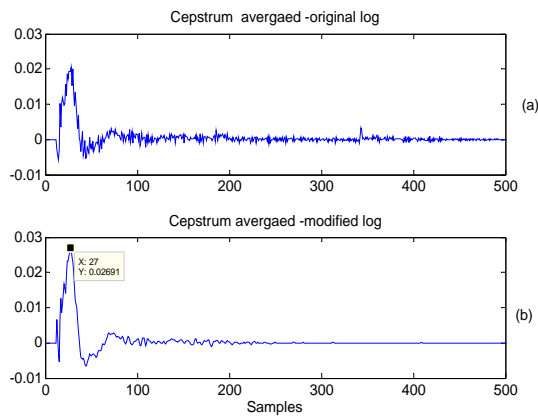


Figure 23 (a) Cepstrum averaged estimate on the original log spectrum (b) Cepstrum averaged estimate on the modified (dynamic range limited) log spectrum

CONCLUSIONS

This paper presents an analytical simulation for the acceleration response of the vibration of a spalled rolling element bearing. The entry into and exit from the spall events are simulated as modified step and impulse responses with precisely known starting times, so as to be able to determine the effects of various simulation and signal processing parameters on the estimated delay times. Two main processing algorithms (joint and separate treatment) were attempted to measure the size of the fault (delay). Both reported good results and corresponded well with measurements from actual signals for a seeded fault. The simulation benefited the algorithms in highlighting the importance of selecting a suitable filter characteristic and pointing to a limitation in using the cepstrum to find the size of the spall, which results mainly from the different nature of the step and impulse responses. An improvement in the results of the cepstrum has been achieved by limiting the dynamic range of the log spectrum used for calculating the cepstrum. The improvement was more noticeable in the separate treatment.

ACKNOWLEDGEMENTS

This work is supported by the Australian Defence Science and Technology Organization (DSTO) as a part of their Centre of Expertise scheme.

REFERENCES

1. M S Darlow, R H Badgley and G W Hogg (1974) 'Application of high frequency resonance techniques for bearing diagnostics in helicopter gearboxes', US Army Air Mobility Research and Development Laboratory, Technical Report, pp. 74-77.
2. P D McFadden and JD Smith, 'Model for the vibration produced by a single point defect', Journal of Sound and Vibration, Vol 96, No 1, pp 69-82, 1984.

3. S Fukata, E H Gad, T Kondou, T Ayabe, and H Tamura, 'On the Vibration of Ball Bearings', Bulletin of JSME, 28 (239), pp 899-904, 1985.
4. Y.T. Su, and S.J. Lin, 'On Initial Fault Detection of a Tapered Roller Bearing: Frequency Domain Analysis', Journal of Sound and Vibration, Vol.155(1), pp 75-84, 1992.
5. D Ho and R B Randall, 'Optimization of bearing diagnostic techniques using simulated and actual bearing fault signals', Mechanical Systems and Signal Processing, Vol 14, No 5, pp 763-788, 2000.
6. J Antoni, and R B Randall, 'A stochastic model for simulation and diagnostics of rolling element bearings with localized faults', Transactions of the ASME, Journal of Vibration and Acoustics, Vol 125, No 3, pp 282-289, 2003.
7. I K Epps, and H McCallion, 'An investigation into the characteristics of vibration excited by discrete faults in rolling element bearings', Annual Conference of the Vibration Association of New Zealand, Christchurch, 1994.
8. N Sawalhi, R B Randall, 'Tracking of spall size in rolling element bearings', paper presented at the sixth International Conference on Condition Monitoring and Machinery Failure Prevention Technologies, Dublin, 23-25 June 2009.
9. N Sawalhi and R B Randall, 'Spectral Kurtosis Enhancement using Autoregressive Models', ACAM conference, Melbourne, Australia, February 2005.
10. N Sawalhi and R B Randall, 'Spectral Kurtosis Optimization for Rolling Element Bearings', ISSPA conference, Sydney, Australia, August 2005.
11. R B Randall and N Sawalhi, "Signal processing techniques for bearing fault size determination" paper presented at the 22nd International Congress and Exhibition on Condition Monitoring and Diagnostic Engineering Management, San Sebastian, Spain June 9 - 11, 2009.
12. RB Randall Frequency Analysis, 3rd ed., Bruel & Kjaer, Naerum, Denmark, 1987.
13. N Sawalhi, R B Randall and H Endo, 'The enhancement of fault detection and diagnosis in rolling element bearings using minimum entropy deconvolution combined with spectral kurtosis', Mechanical Systems and Signal Processing, 21(6) pp. 2616-2633, August 2007.